2-7-2023

Modeling and Analysis of the Intrinsic Cardiac Nervous System in Closed-Loop Cardiovascular Control

Michelle M. Gee
Thomas Jefferson University

Abraham M. Lenhoff

James S. Schwaber
Thomas Jefferson University

Babatunde A. Ogunnaike

Rajanikanth Vadigepalli
Thomas Jefferson University

Available online at www.sciencedirect.com

ScienceDirect

IFAC PapersOnline CONFERENCE PAPER ARCHIVE

IFAC PapersOnLine 55-23 (2022) 146–147

Modeling and Analysis of the Intrinsic Cardiac Nervous System in Closed-Loop Cardiovascular Control

Michelle M. Gee [*,**] **Abraham M. Lenhoff** [*]
James S. Schwaber [**] **Babatunde A. Ogunnaike** [*,⋆]
Rajanikanth Vadigepalli [**]

[*] *Department of Chemical and Biomolecular Engineering, University of Delaware, Newark, DE 19716 USA*
[**] *Daniel Baugh Institute for Functional Genomics and Computational Biology, Department of Pathology, Anatomy and Cell Biology, Thomas Jefferson University, Philadelphia, PA 19107 USA (e-mail: rajanikanth.vadigepalli@jefferson.edu)*

Abstract: The baroreceptor reflex is a multi-input, multi-output physiological control system that regulates short-term blood pressure by modulating nerve activity between the brainstem and the heart. The computational model by Park et al. (2020) is the most recent iteration in our exploration of the system. However, the contributions of "the little brain of the heart", the intrinsic cardiac nervous system (ICN), to local control of the heart and to the integration of sensory information is unknown and has been overlooked in previous models. We have incorporated a high-fidelity representation of the ICN into a model of the baroreceptor reflex based on anatomical, molecular, and physiological evidence. The model consists of (1) differential equations to represent the cardiovascular system, and (2) transfer functions to represent neural control components, connected in a closed-loop control circuit. We use the model to evaluate the impact of alternative ICN network structures on overall cardiovascular control in response to mean arterial pressure and lung tidal volume perturbations. Our results show that the local circuit neurons that integrate sensory information into the ICN strengthen the response of ICN neuron activity, especially at low blood pressures, suggesting that the ICN amplifies the brainstem's response to perturbations.

Keywords: Estimation and control in biological systems, physiological modeling, cardiovascular, baroreceptor reflex, vagus nerve

1. INTRODUCTION

Existing models of cardiac control have sought to recapitulate the autonomic dysfunction associated with cardiovascular disease, but have ignored the intrinsic cardiac nervous system (ICN) (Park et al., 2020). While previously thought to be a relay station, new data suggests the ICN integrates local cardiac reflexes and central nervous system inputs. We present a model of autonomic control of the heart that incorporates ICN electrophysiological data and use it to probe the role of the local reflex in cardiac control.

2. MODEL IMPLEMENTATION

2.1 Model Structure

The model is based on prior work by Park et al. (2020) with the addition of the ICN to explore the role of the local cardiac reflex. It consists of two main parts: (1) the cardiovascular system, represented by ordinary differential equations derived from mass balances of blood flow through body compartments, and (2) the neural sensing and control system, represented by sigmoidal functions representing the saturating firing behavior of neurons (Figure 1). The cardiovascular system model includes representations of the pulmonary and systemic circulatory systems and a pulsatile model of the heart. The neural portion of the model includes representations of sensory, brainstem, and ICN neuronal groups.

2.2 Parameter Estimation

For the portions of the model that were based upon the model of Park et al. (2020), we used existing model parameters. The remaining parameter values were selected to produce simulations that matched experimental data associated with cardiovascular and ICN electrophysiological behavior (Rajendran et al., 2019) or were estimated from experimental data (Iano et al., 1973). To select sets of parameter values to describe plausible behavior of ICN neurons, we adapted the parameter estimation strategy used by Park et al. (2020). We selected parameter sets via

⋆ This work is in memory of Dr. Babatunde A. Ogunnaike, who co-advised MG and guided the model development and analysis. Funding was provided by NIH U01-HL133360, NIH OT2-OD030534, and NSF 1940700. Computational resources from the DARWIN project at the University of Delaware are made possible by NSF OAC-1919839.

10.1016/j.ifacol.2023.01.031

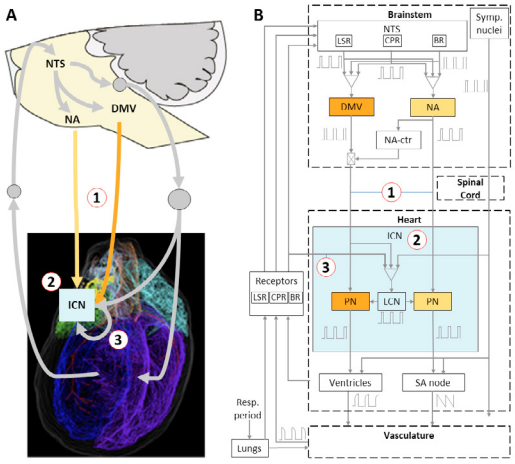

Fig. 1. Anatomical (A) and block diagram (B) schematics of neural control of the heart. Of note are (1) two lanes of vagal innervation and (2) the ICN as the controller for an inner loop that integrates (3) sensory information for the local cardiac reflex. The model contains three types of sensors: baroreceptors (BR), cardiopulmonary receptors (CPR), and lung stretch receptors (LSR). These sensory inputs are integrated in the nucleus tractus solitarius (NTS), which has three subgroups representing neuronal subtypes with different afferent inputs corresponding to the three receptor types. The NTS projects to the nucleus ambiguus (NA) and the dorsal motor nucleus of the vagus (DMV), the two primary lanes of vagal outflow to the heart. These two lanes innervate separate populations of principal neurons (PN) in the ICN. PNs also receive input from local circuit neurons (LCN), which integrate local cardiac afferent feedback. ICN activity controls the sinoatrial (SA) node and ventricles which contribute to heart rate and blood pressure respectively in the cardiovascular system model. Heart image adapted from Achanta et al. (2020).

Sobol sampling within a parameter space constrained to a $\pm$ 5 fold range of similar parameters for neuronal subtypes and to within the range of experimentally observed ICN firing frequency (Rajendran et al., 2019). We then selected the best parameter set based on the sum of mean square errors of heart rate, elastance, and ICN firing frequencies.

3. RESULTS

The pressure-volume loop and cardiovascular metrics in Figure 2 match the results of previous models (Park et al., 2020). The model without a local reflex predicts slightly higher blood pressures, but overall the models have similar behavior in the absence of a perturbation because the effect of the local reflex is weakened by the LCNs.

Figure 3 shows that the model with a local reflex is able to maintain similar or lower heart rate and elastance values, suggesting that removing the local reflex increases elastance and disrupts the system's ability to control heart rate, especially at lower blood pressures and higher lung tidal volumes. The local reflex becomes significant at high lung tidal volumes and its removal attenuates the sensitivity of the elastance response to perturbations.

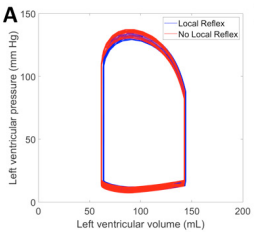

B

Parameter	Local Reflex	No Local Reflex	Healthy Range
Systolic Pressure (mm Hg)	126	128	90-130
Diastolic Pressure (mm Hg)	79	79	60-80
Heart Rate (bpm)	61	62	60-100
Cardiac Output (mL/s)	83	83	83-100
Ejection Fraction (–)	0.55	0.57	0.50-0.75

Fig. 2. Closed-loop model predictions of pressure-volume loops and cardiovascular metrics for healthy people with (blue) and without a local reflex (red).

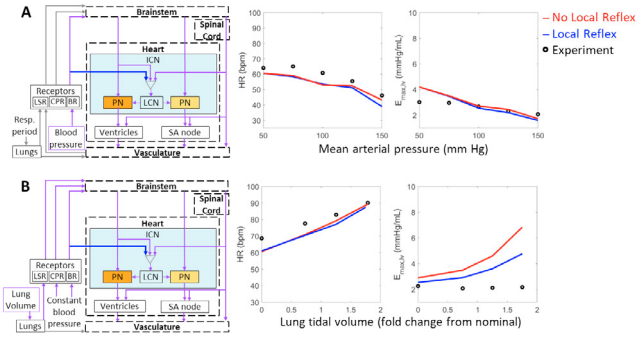

Fig. 3. Heart rate and left ventricular elastance ($Emax_{lv}$) responses to mean arterial pressure (A) and lung tidal volume (B) changes for models with (blue) and without (red) a local reflex compared to averages from experimental data (black) (Suga et al., 1976; Greenwood et al., 1980). Open-loop simulations were performed to match the experimental conditions. Purple lines in the diagrams highlight information flow through models with and without a local reflex, while blue lines are present only in the model with a local reflex. Baseline heart rates and elastances of 61.2 bpm and 2.695 mm Hg/mL (A) and 84.6 bpm and 2.392 mm Hg/mL (B) were used (Park et al., 2020).

REFERENCES

Achanta, S., Gorky, J., Leung, C., Moss, A., Robbins, S., Eisenman, L., Chen, J., Tappan, S., Heal, M., Farahani, N., Huffman, T., England, S., Cheng, Z.J., Vadigepalli, R., and Schwaber, J.S. (2020). A comprehensive integrated anatomical and molecular atlas of rat intrinsic cardiac nervous system. *iScience*, 23(6), 101140.

Greenwood, P.V., Hainsworth, R., Karim, F., Morrison, G.W., and Sofola, O.A. (1980). Reflex inotropic responses of the heart from lung inflation in anaesthetized dogs. *Pflugers Arch.*, 386(2), 199–205.

Iano, T.L., Levy, M.N., and Lee, M.H. (1973). An accelerator component of the parasympathetic control of heart rate. *Am. J. Physiol.*, 224(5), 997–1005.

Park, J.H., Gorky, J., Ogunnaike, B., Vadigepalli, R., and Schwaber, J.S. (2020). Investigating the effects of brainstem neuronal adaptation on cardiovascular homeostasis. *Front. Neurosci.*, 14, 470.

Rajendran, P., Vaseghi, M., and Ardell, J. (2019). Functional recordings from the pig intrinsic cardiac nervous system (ICN). doi:10.26275/OWRI-MPSX.

Suga, H., Sagawa, K., and Kostiuk, D.P. (1976). Controls of ventricular contractility assessed by pressure-volume ratio, emax. *Cardiovasc. Res.*, 10(5), 582–592.